PHYSICAL REVIEW D VOLUME 25, NUMBER 11 1 JUNE 1982

Delayed energetic events in extensive air showers

P. N. Bhat, S. K. Gupta, P. V. Ramana Murthy, B. V. Sreekantan,
S. C. Tonwar,* and P. R. Viswanath
Tata Institute of Fundamental Research, Homi Bhabha Marg, Colaba, Bombay 400 005, India
(Received 22 January 1982)

Production of massive (≥ 10 GeV/c^2) strongly interacting particles in very-high-energy interactions has been suggested by many theories. These particles, if produced in the cores of extensive air showers in the upper atmosphere, would arrive at the observational level delayed by tens of nanoseconds relative to all other known particles of similar energy, provided they are relatively stable (lifetime $> 10^{-6}$ s). Experiments searching for such particles have reported observing delayed (> 20 ns) energetic (> 40 GeV) events. However several anomalous features observed for these events have precluded their interpretation in terms of massive particles with ordinary hadronic interaction characteristics in a conclusive manner. We report here the details of a new experiment carried out at the Ooty laboratory during 1978–1981 where we have attempted to study the delayed energetic events with a multidetector system placed inside the large Ooty multiplate cloud chamber. Our observations show that the delayed energetic events could not be ascribed to high-energy hadronlike interactions of a massive strongly interacting particle. We have observed one delayed event showing a high-energy cascade in cloud chamber but inadequate timing information does not make a convincing case for this event to be due to a high-energy delayed massive hadron. However this event combined with observation of two similar events earlier by Tonwar *et al.* suggest the existence of some interesting phenomenon requiring observations over a long period of time. We have obtained a 99%-C.L. upper limit of 1.7×10^{-11} cm^{-2} s^{-1} sr^{-1} for the flux of massive particles in extensive air showers of size $\sim(5\times10^4)-(5\times10^6)$ particles which corresponds to an upper limit of 2.5×10^{-33} cm^2 for the production cross section for particles of mass > 10 GeV/c^2 at energies of $\sim10^5-10^7$ GeV.

I. INTRODUCTION

Experimental searches for massive particles[1] which may be produced in high-energy particle interactions occurring in the cores of extensive air showers have given interesting but inconclusive results. The large arrival delay expected[2] for a massive particle in traveling through the atmosphere relative to the shower electrons has been used by these experiments[3–8] as the signature for identification. The delay Δt is related to the mass (m) and energy (E) of the particle through the simple relation

$$\Delta t \sim (h/\beta c - h/c)$$
$$\sim 1667(hm^2/E^2)\ \text{ns};\quad \beta = v/c\ ,$$

where v is the velocity of the massive particle, c is the velocity of light, and h is the distance traveled by the particle in the atmosphere in kilometers. Since the expected delays per kilometer for energetic (> 40 GeV) pions, kaons, and nucleons are less than 0.02, 0.25, and 0.92 ns, respectively, a delay of 20 ns or more requires these particles to travel more than 22 km without decay or interaction which is highly unlikely. In fact, detailed Monte Carlo simulation[5] of extensive air showers initiated by protons and iron nuclei of energy 10^5-10^6 GeV have shown that the probability of a hadron observed at mountain altitude (800 g cm^{-2}) to have these delay and energy characteristics due to fluctuations is much smaller than 10^{-4}.

All five experiments[3–7] to date have reported observing events with these delay-energy characteristics. However these observations could not be regarded as conclusive evidence for the existence of massive particles due to the absence of enough detailed information about the events and due to the unusual nature of these events. For example, experiments[3–5] using deep multilayer calorimeters to measure the energy of the hadrons showed that the delayed energetic events did not penetrate thick

layers of absorbers and most of the ionization deposited in the calorimeter was confined to a region close to one of the sampling detectors. Tonwar *et al.*[6] attempted to observe the cascades for these events by placing the timing detector inside the large multiplate cloud chamber. They reported two events showing well developed cascades in the cloud chamber with energy larger than 30 GeV and with delay of more than 20 ns. Goodman *et al.*[7] attempted to observe the delayed hadrons with wide-gap spark chambers located on both sides of the hadron timing detector inside the calorimeter, but separated by $\sim 120\ \mathrm{g\,cm^{-2}}$ of iron. They have reported observing three delayed energetic events, but their cascades could not be distinguished clearly in the spark-chamber pictures. However, in both of these experiments the timing information was provided by only one detector.

We report here the results from a new experiment carried out at the Ooty laboratory (altitude $800\ \mathrm{g\,cm^{-2}}$) during 1978–1981, where we attempted to overcome some of the problems faced by the earlier experiments. The major improvement in our experiment is in the use of two well separated timing detectors inside an absorber assembly. As in the experiment of Tonwar *et al.*[6] we placed the hadron timing detectors inside the Ooty multiplate cloud chamber which permits a detailed visual study of the hadron cascades going through the timing detectors. These detectors are placed at two depths in the multiplate assembly and provide unambiguous measurement of the delay for the hadron. Since the more numerous prompt lower-energy hadrons can suppress the detection of some of the delayed hadrons near the cores of air showers, separate timing measurements have been made for lower and higher pulse heights for the timing detectors in the present experiment. These and other details of the experimental system, data collection, and data analysis are given in the next section. The experimental results are presented in Sec. III and their interpretation is discussed in Sec. IV along with the discussion of results from earlier experiments. Conclusions are presented in Sec. V.

II. EXPERIMENTAL DETAILS

A. Experimental system

The apparatus consisted of a hadron-detection and -timing system, a shower-front timing system, and an air-shower array. The hadron-detection system is composed of a pair of thin (1 cm) plastic scintillation detectors S_3 and S_4, each of area $0.8\times0.8\ \mathrm{m^2}$ and viewed through an adiabatic light pipe by a RCA 8575 photomultiplier. These two detectors are placed inside the multiplate assembly of the large ($2\ \mathrm{m}\times1.5\ \mathrm{m}\times1\ \mathrm{m}$) cloud chamber as shown in Fig. 1. The absorber above S_3 consisted of $112\ \mathrm{g\,cm^{-2}}$ of iron in the form of eight plates (including the top wall of the chamber), a thin layer of iron ($5\ \mathrm{g\,cm^{-2}}$), and a layer of lead of thickness $43\ \mathrm{g\,cm^{-2}}$. The lower detector S_4 was separated by $56\ \mathrm{g\,cm^{-2}}$ of iron and 60 cm of space relative to S_3 in the first part of the experiment. In the second part of the experiment the detector S_4 was placed above S_3 by removing one of the iron plates above S_3. In this configuration the two detectors were separated by only $3\ \mathrm{g\,cm^{-2}}$ of matter (plywood and aluminum) and 15 cm of space vertically. In the first part, the absorber assembly above S_3 offered 16 radiation lengths or about 1.2 interaction mean free paths for the development of electron-photon cascades and nucleon interaction, respectively. The lead-layer shielding above the chamber was basically for preventing the low-energy shower particles from entering the chamber for near vertical ($\theta<25°$) showers. For larger-angle showers the lead shielding was not effective, but the iron plates above S_3 provided some measure of shielding. It may be noted that the incidence of some larger-angle shower particles on S_3 or S_4 does not cause much difficulty since these are mostly prompt particles and are unlikely to simulate a delayed energetic event. However, these particles can prevent, in some cases, the detection of the delayed event by triggering the timing system earlier.

The shower front was timed by six detectors. Two of these, S_1 and S_2, were placed above the

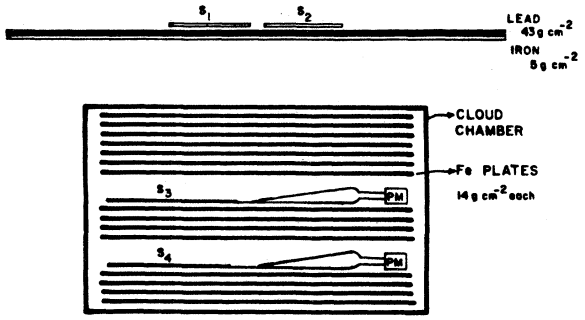

FIG. 1. A schematic diagram of the experimental system for the detection and timing of the shower front and the hadron.

shielding of the cloud chamber (Fig. 1). These detectors, plastic scintillators each 0.5×0.5 m^2 in area and 5 cm thick, are also viewed by RCA 8575 photomultipliers. These detectors measured the shower density above the chamber and provided the timing reference for measurement of the delays for the signals from S_3 and S_4. The other four detectors, N, E, W, and S, were liquid scintillation detectors, each 1 m^2 in area, which were placed at distances of $5-15$ m from the chamber. These provided the measurement of relative arrival times for the shower front for computation of the shower arrival direction. The lateral distribution of shower particles was measured by 20 density detectors (plastic scintillators) spread over an area of radius ~40 m around the cloud chamber, which enabled determination of the core position, age, and the size for each shower.

B. Data selection and recording

The data selection and recording system is shown schematically in Fig. 2. The pulses from each of the shower detectors S_1 and S_2 were fed after passive splitting to a discriminator and after further splitting to 2 of the 12 channels of the 10-bit analog-to-digital-converter (ADO) (CAMAC) module. The pulses from each of the hadron detectors S_3 and S_4 were fed after passive splitting to a discriminator (lower threshold, 100 mV) and after further splitting to another discriminator

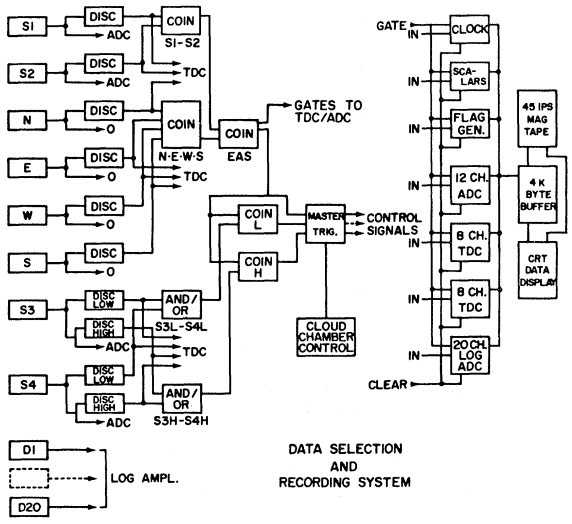

FIG. 2. A schematic diagram of the data selection and recording system.

(higher threshold, 250 mV) and after another splitting to two channels of the ADC module. One of the two pulses going to the ADC module for each detector was attenuated by a factor of 5 to extend the range of measurement of the number of particles in these detectors. The pulses from each of other shower-timing detectors were fed after passive splitting to a discriminator and the other output of the splitter was used for a different experiment. The pulses from each of the discriminators mentioned above were fed to the 11-bit time-to-digital converter TDC (CAMAC) module for measuring their arrival times relative to the START gate. The pulses from the density detectors (D_1 to D_{20}) were fed directly to the gated logarithmic amplifier digitizer system with capability of measuring particle densities in the range of $1-5000$ m^{-2}.

The event selection was carried out through a three-step coincidence system. First a twofold coincidence between the signals from the discriminators for S_1 and S_2 was generated. The discrimination level was changed during the experiment, as will be discussed later. Separately, a fourfold coincidence of the signals discriminated at the single-particle level from the detectors N, E, W, and S was generated. The extensive-air-shower (EAS) selection was then completed by requiring a coincidence between the output pulses from the $(S_1\cdot S_2)$ and $(N\cdot E\cdot W\cdot S)$ coincidence modules. This shower trigger served as the prompt START gate to all the data modules. By arranging suitable delays it was ensured that the timing of this gate was always determined by $(S_1\cdot S_2)$. This scheme was necessary to avoid any delay for the START gates to the TDC and ADC modules due to the arrival angle of the shower. The hadron was selected by either requiring a signal above a preset level (low or high) in either S_3 or S_4, or by requiring a twofold coincidence between these pulses. As discussed later these different selection conditions were used at different times to study specific problems. Finally a master trigger was generated by requiring a coincidence between the shower (EAS) pulse and the hadron $(S_3\cdot S_4$ or $S_3/S_4)$ pulse which transferred the data from various modules (clock, scalers, flag generators, ADC's, TDC's, and logarithmic ADC's) to the magnetic tape recording system through a 4000-byte-capacity data buffer module. An inspection of part of the data could be done by transferring it from either the buffer or the magnetic to the video (cathode-ray-tube) data-display system. The shower pulse which served as a START gate also generated a clear gate for all the

modules if it was not followed within 250 ns by a master trigger. The master trigger also gave the trigger for the cloud chamber control system. Since the dead time for the chamber after every trigger is rather long (~ 10 min) only triggers having either a high-energy (>20 GeV) or a delayed (>5 ns) hadron in the hadron-detection system were allowed to proceed to the chamber control system. All the detectors were routinely calibrated using near-vertical atmospheric muons.

Data were collected with different selection criteria to search for delayed energetic events in different regions of air showers and for different conditions for the energy loss in the hadron detectors. A summary of various triggers used, the run time, and the number of events collected for each of these triggers is given in Table I. Initially (part 1a) the search was restricted to regions close to the shower core by requiring a particle density ≥ 12 m^{-2} over the chamber, that is, requiring ≥ 3 particles in both S_1 and S_2. The threshold for the discriminators for S_3 and S_4 was kept at about four particles and a coincidence was required between these two detectors. During this period the signals from S_3 and S_4 were not discriminated at the higher threshold levels and therefore only the arrival times of the first signals in S_3 and S_4 which crossed the four-particle level were measured. Since some delayed particles could be masked by lower-energy hadrons arriving earlier the threshold for the discriminators was later raised (part 1b) to about 20 particles (note that during this period there were no measurements for the arrival times at the lower particle level). It was soon realized that due to fluctuations in the development of cascades in the absorber assembly, the average hadron energy required for giving ≥ 20 particle signals in both S_3 and S_4 could be considerably larger than about 30—40 GeV. Therefore during part 1c of the experiment separate discriminators with lower (5 particles) and higher (25 particles) thresholds were installed for both S_3 and S_4 and arrival times were measured independently at these two levels. In this part the hadron selection required only signals larger than about five particles in both the hadron detectors. Finally, in part 1d the requirement of a coincidence between the signals from S_3 and S_4 was removed and the hadron selection required only a signal >5 particles in either of these two detectors. Also the search for the delayed energetic events was extended to farther distances from the shower core by reducing the shower density requirements from 12 m^{-2} to only 4 m^{-2} over the cloud chamber in part 1d of the experiment. It may be noted that events selected with any of the triggers in parts 1a, b, or c were part of the sample selected with the criteria adopted in part 1d. However this relaxation in selection criteria also permitted a study of delayed energetic events which, for some reason, may give a signal only in one of the hadron detectors.

Since many events observed in the first part of the experiment showed signals only in one of the two detectors, the absorber thickness between S_3 and S_4 was reduced from 56 g cm^{-2} to about 3 g cm^{-2} in the second part of the experiment. As mentioned earlier this was achieved by placing the detector S_4 above S_3 with only thin aluminum and plywood sheets between them. In part 2a the selection conditions were kept similar to those in part 1d. Then for a short run (part 2b) data was collected with a higher shower density (12 m^{-2}) requirement. However, in the second part of the experiment there was no information available from the cloud chamber since a major fire accident in the high-voltage flashing system for the chamber had forced the shutdown of the operation of the chamber.

TABLE I. Summary of data collection.

Part	Trigger	Shower-detectors threshold (particles)	Hadron-detectors threshold (particles)	Operational time (h)	Number of events
1a	EAS·(S_3·S_4)	3	4	1596	26785
1b	EAS·(S_3·S_4)	3	20	1348	5338
1c	EAS·(S_3·S_4)	3	5	2318	24419
1d	EAS·(S_3/S_4)	1	5	3595	128131
2a	EAS·(S_3/S_4)	1	5	1920	64407
2b	EAS·(S_3/S_4)	3	5	846	17284

C. Data analysis

The observed signals from all the detectors were converted to equivalent numbers of particles using the calibration values obtained for muons. The relative arrival times from the shower timing detectors were used to compute the arrival direction of the shower. From the observed distribution of the arrival times from detectors placed adjacent to each other it was estimated that the error in the determination of the zenith angle of a shower is $\sim 4°$. The particle densities observed in density detectors were fitted to a lateral distribution function[9] to obtain the position of the shower core, the age parameter, and the shower size. The errors in the determination of the position of the shower core, age, and the size have been estimated from analysis of artifical showers[9] to be 1 m, ± 0.1 and $\pm 30\%$, respectively.

The arrival delay of the signal in S_3 and S_4 relative to shower particles in S_1 or S_2 can be obtained, in principle, from the difference in observed TDC counts (2 counts/ns) after subtracting the effects due to different transit times (cables, electronics, etc.) in these detector systems. Since the rise times (10–90% ampiltude) of the pulses going to discriminators are about 5 ns, a direct determination of transit times using near-vertical muons was not considered to be very useful. Therefore the transit times have been determined from the medians of the distributions for various TDC channels for showers with very high density (>400 m^{-2}) over the chamber and very-high-energy (>100 particles) hadrons through S_3 and S_4. As expected from slewing due to rise time these medians shift by as much as 4 ns for small signals in these detectors. Although such a trend is also expected due to physical processes (lower-energy electrons or hadrons ariving a little delayed, on the average) it is not possible to distinguish between these two effects in this experiment. Since S_1 or S_2 provide the START gate for the TDC's the delay ΔT of the signal in S_3 or S_4 is determined from the relation

$$\Delta T = [T(S_3/S_4) - T_m(S_3/S_4)] - [T(S_1/S_2) - T_m(S_1/S_2)] .$$

Here $T(S_3/S_4)$ and $T(S_1/S_2)$ are the arrivial times for signals measured by TDC's for S_3 or S_4 and S_1 or S_2, respectively. T_m's are the medians for the distributions for these detectors. Since one of the shower detectors may be delayed sometimes due to fluctuations, the delays are measured relative to the earlier of these two detectors.

The time resolution for these detectors has been measured by observing the distribution of the difference in arrival times between the detectors placed above one another with no absorber above or between them. It has been observed that this distribution is nearly Gaussian with a standard deviation (σ) of about 3 ns for single particles. The distributions are narrower ($\sigma \sim 2$ ns) for signals larger than five particles. Therefore an individual high-energy event with measured delay, e.g., 10 ns, in one detector only cannot be considered very significant but it acquires importance if delays measured by both detectors S_3 and S_4 relative to both shower detectors S_1 and S_2 are larger than 10 ns. On the other hand delays larger than 20 ns in even one detector are difficult to account in terms of instrumental fluctuations. It should be noted that fluctuations in the arrival time of the shower front only reduce the measured delay of the hadron and do not lead to an overestimate of the hadron delay. These fluctuations, in fact, lead occasionally to an apparent small negative delay for the hadrons as would be seen from the delay distributions presented in the next section.

It is rather difficult to estimate accurately the energy of the hadrons from the amplitude of the signals in S_3 and S_4 except for those events which have a cloud-chamber picture showing a well developed cascade. Since cloud-chamber pictures were available only for a small fraction of the events due to various inefficiencies in the operation of cloud chamber, the hadron detectors S_3 and S_4 have been treated here as burst detectors. An average conversion factor of 1 GeV per particle in S_3 or S_4 has been used to estimate the energy of the hadron. This conversion factor is based on observations of hadron cascades in calorimeters[10] and Monte Carlo simulations.[10,11] In individual cascades large fluctuations can be expected, leading to an uncertainty in energy by about a factor of 2. However, in most of the results presented in the next section no conversion to energy has been made. Since the observations in this experiment were mostly in regions close to the shower core, within about 20 m, it is expected[12] that many events would have contamination from the large background due to low-energy particles (muons, hadrons, or electron cascades from above or sides). However, this contamination is important only for nondelayed events where it cannot be distinguished from the contribution due to the prompt high-energy hadron. In case of events with delayed hadrons this contamination, mostly time-coincident

with shower front, causes the low-threshold timing channel to show a prompt signal. In cases where this contamination is large enough to trigger the high-threshold timing channel the delayed event cannot be identified.

The main purpose for the use of the cloud chamber in this experiment was to obtain a better estimate of the energy for the delayed energetic events since cascade development and absorption could be visually studied in detail. The energy of a cascade seen in the multiplate cloud chamber can be estimated with good accuracy ($\pm 30\%$) from the track-length integral using the conversion factor obtained from calculations.[11] For a part of the data cloud-chamber pictures were scanned to compare the signals observed in detectors S_3 or S_4 with the number of particles seen visually in the picture. It has been observed[12] that for events with a smaller (<30 particles) signal there was good agreement between the two methods. However, for larger signals the number of particles given by S_3 or S_4 were mostly larger than the numbers seen visually. This is expected since slow particles (evaporation fragments) and particles traversing the detectors at large angles give a large signal in the scintillation detector. This has also been seen in accelerator experiments[10] and is, in fact, one of the main reasons for the large error in the estimation of energy from observed bursts.

III. EXPERIMENTAL RESULTS

The following information was available for each event after the analysis of the data: (i) Observed signal in detectors S_1, S_2, S_3, and S_4 in terms of equivalent number of particles, (ii) arrival delays of the signals in S_3 and S_4 relative to the shower front at two threshold levels, except in parts 1a and b of the experiment, (iii) arrival angles, core position, age, and shower size for most of the showers except for about 10% of the events whose shower information was not useful for various reasons, and (iv) cloud-chamber pictures for a small fraction of the high-energy events.

Since earlier experiments[3–7] have all observed delayed energetic events with basically a single hadron detector it is of interest to study first the delay distributions in the present experiment by treating S_3 and S_4 as independent detectors. Figure 3(a) shows the diplot of the number of particles against the arrival delay of the signal in S_3 for all events collected in the first part of the experiment. A similar plot for S_4 is shown in Fig. 3(b). These

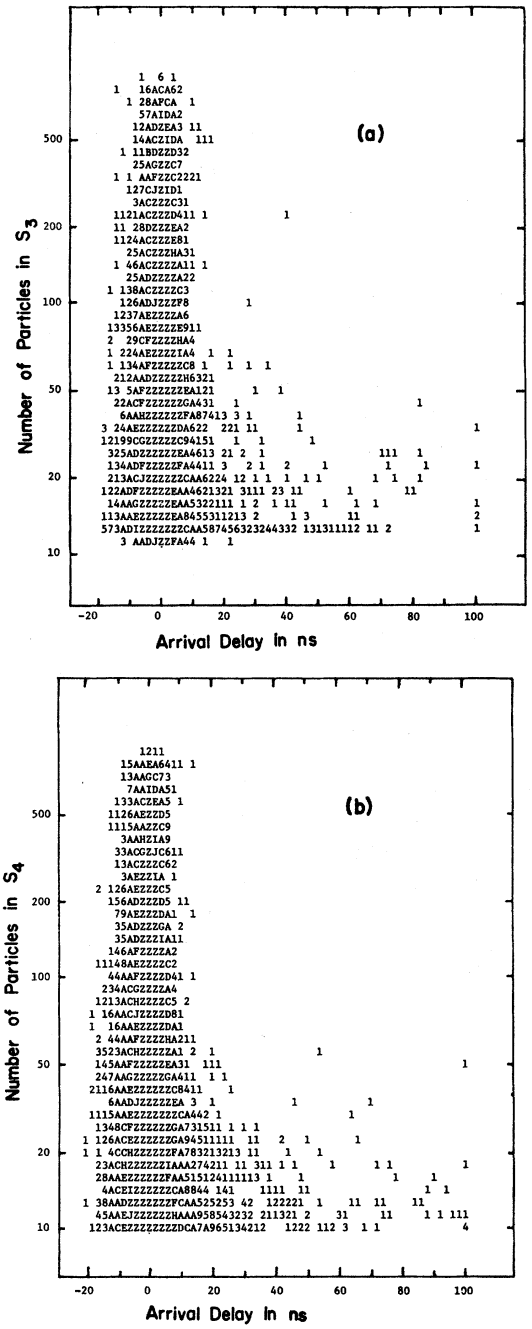

FIG. 3. Diplot of the number of particles (N) and the arrival delay in nanoseconds of the signal in (a) S_3 and (b) S_4 for events with $N \geq 10$ particles and shower density ≥ 4 m^{-2} in part 1 of the experiment (in all diplots A represents 10–19 events, B represents 20–29 events, etc., and Z represents ≥ 100 events).

diplots show a number of delayed energetic events (delay >20 ns, number of particle >40) very similar to events observed in earlier experiments.

The correlation between the time delays mea-

sured by the detectors S_3 and S_4 is shown in Fig. 4 for the events shown in Figs. 3(a) and 3(b). As mentioned earlier most of these events (except in part 1b) required for selection five particles or more in S_3 and S_4. It is interesting to see from this figure that there are basically two types of delayed events. The first type, called type A here, is populating the diagonal region in Fig. 4 and the delays measured by S_3 and S_4 for this type of events are in good agreement with each other (± 5 ns). In the other type of events, labeled type B here, which lie along the axes in Fig. 4, the signal from only one of the two detectors is delayed. It is evident that while type A events are likely to be due to cascades traversing both the hadron detectors, the type B events are certainly due to passage of different cascades through S_3 and S_4. Apart from these two types of events there is another class of events, called type C here, which was studied in part 1d and parts 2a and b of the experiment. These events are characterized by the presence of a signal in only one of the two hadron detectors and only one measurement of arrival delay was available for these events. Table II gives the summary of the data for the operating time, number of events, event rate, and relative frequencies for different types of events with different selection thresholds in both parts of the experiment. Since relative rates for different types of events were not very sensitively related to the shower-density thresholds used here, data collected with different triggers in part 1 have been combined together for computation of the rates and frequencies given in Table II. It is seen from this table that type C events, which are mostly due to low-energy hadrons, are the more common type of events among those selected with lower-threshold trigger. As expected for higher-energy events, type A events form the majority of events selected with

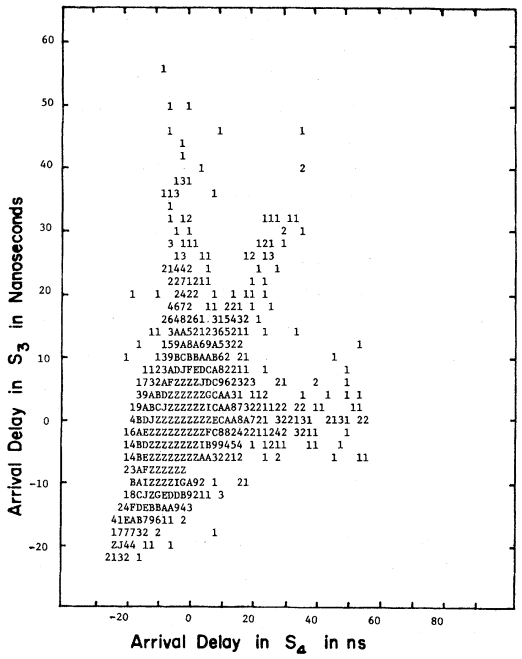

FIG. 4. Correlation between the delay of the signal in S_3 and S_4 (part 1).

TABLE II. Operational time, number of events, event rate, and relative frequencies for various types of events.

Part	Hadron-selection threshold	Event type	Operational time (h)	Number of events	Event rate (h^{-1})	Relative frequency
1	Low	A	7509	62 024	8.26	0.26
		B	7509	22 174	2.95	0.09
		C	3595	74 753	20.79	0.65
1	High	A	7261	23 127	3.18	0.76
		B	7261	2 143	0.29	0.07
		C	3595	2 550	0.71	0.17
2	Low	A	2766	29 644	10.70	0.41
		B	2766	7 672	2.77	0.11
		C	2766	34 980	12.65	0.48
2	High	A	2766	9 001	3.25	0.96
		B	2766	280	0.10	0.03
		C	2766	114	0.04	0.01

the higher-threshold trigger. It may be noted that some of the type C events are, in fact, type A events whose cascades have missed the other detector due to particular combination of position and angle of the cascades.

With the aid of two channels for each of the hadron detectors for measuring the arrival times at two different threshold levels, it was possible in this experiment to distinguish between two hadrons arriving at different times on the same detector. A diplot of the arrival delays measured by the lower-threshold and the higher-threshold channels of a detector is shown in Fig. 5. It is seen that there are many events where a low-level signal which was time-coincident with the shower front has been followed by a delayed high-level signal in the detector. This capability makes it possible to search for delayed energetic events near cores of showers where a large background of low-energy hadrons is expected. However if the hadron arriving earlier has higher energy, then the delay of a subsequent hadron is not recorded.

A. Type A events

A detailed study of events of type A in which the delays measured by S_3 and S_4 agree to within 5 ns forms the most significant part of this experiment. Figure 6(a) shows the diplot of the number of particles and the delay for type A events collected in part 1 of the experiment. It is quite clear from this figure that there are no large-delay (>20 ns) high-energy (>40 particles) events in this data. However there are a few marginally interesting events with delays in the 10—20 ns range which have signals of 40 particles or more in one of the hadron detectors. The details of these events are given in Table III.

For a study of events which are more likely to

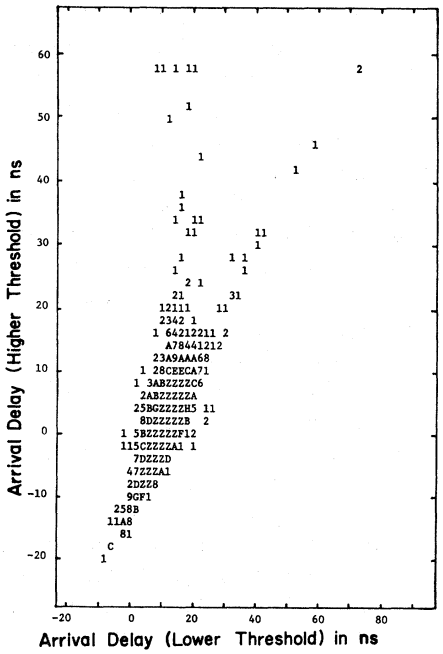

FIG. 5. Correlation between the delays measured by S_3 or S_4 at lower (≥ 5 particles) and higher (≥ 25 particles) threshold levels (part 1).

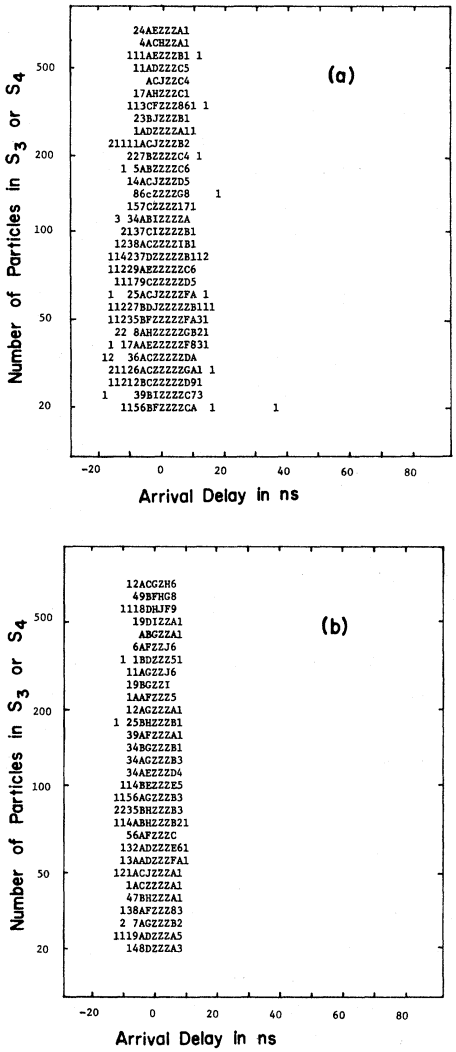

FIG. 6. Diplot of the number of particles and the arrival delay for (a) all type A events and (b) type A events which show good agreement, within 3 ns, between time measured at lower- and higher-threshold levels (part 1).

TABLE III. Characteristics of delayed energetic events of type A.

Serial number	Event identification number	$10^{-4}\times$Shower size	Shower density (m^{-2})	Shower core distance (m)	Shower arrival angle (deg)	Number of particles S_3	Number of particles S_4	Arrival delay (ns) S_{3L}	Arrival delay (ns) S_{3H}	Arrival delay (ns) S_{4L}	Arrival delay (ns) S_{4H}	Event type
1	39736	71	40	28	35	10	57	16		16		A
2	112264	26	52	6	8	47	18	14	13	15	15	A
3	176685	14	68	4	15	151	31	16	17	16	19	A
4	220045	77	16	42	42	52	9	12	15	14		A
5	220917	28	360	1	23	346	205	14	15	14	14	A
6	245114	999	840	6	16	52	37	4	18	5	15	A
7	248967	42	80	8	31	47	12	9	15	12		A
8	251891	54	440	8	26	57	88	11	16	14	15	A
9	273421	64	640	3	35	86	27	11	15	13		A

be due to single well-defined cascades traversing both detectors, another selection condition could be imposed on type A events. This condition requires a good agreement (± 3 ns) between the arrival times measured at lower and higher thresholds. The dispersion in the measurement of delays due to fluctuation in arrival time for the shower front was reduced by requiring a good agreement (± 2 ns) between arrival times measured by S_1 and S_2. Figure 6(b) shows the diplot for events satisfying these rather strict selection conditions. As seen from this figure the time distribution has become noticeably narrow with hardly any event with delay larger than 8 ns. This figure also shows that the use of two detectors for measuring the arrival time of a hadron cascade is very effective for identification of a genuinely delayed hadron for delays larger than 10 ns.

Of all events with 50 particles or more in one of the hadron detectors cloud-chamber pictures were available for 1350 events ($\sim 5\%$). A scan of these pictures revealed that 1287 events were type A showing at least one hadron cascade that traversed both the detectors. The other 63 events were type B or C events. Some of the type C events also showed a good cascade in the chamber but the cascade traversed only one detector and missed the other due to the particular configuration of its position and angle. Interestingly 47% of the type A events had more than one cascade traversing both the detectors. Also the events with multiple hadron cascades had the shower core nearer to the chamber compared with single-hadron-cascade events. Examples of different types of events discussed above are shown in Fig. 7.

A study of the correlations of delayed events with various parameters characterizing associated showers like size, core distance, etc., would give a better understanding of the production process for the particles responsible for these events. However since there are no large-delay high-energy events observed among type A events we do not discuss here the dependence of delay distribution on various shower parameters.

B. Type B and type C events

As discussed earlier, events of type B are more likely due to two hadrons with different arrival delays. One of these hadrons is usually time-coincident with the shower front and may have given a signal in one or both of the hadron detectors. The other particle is delayed and its signal is observed in only one of the detectors. On the other hand, the type C event could be due to one or two hadrons but the signal is observed in only one detector. For type C event the lower-energy hadron is also usually time-coincident with the shower front. In some cases the earlier signal in either type B or C might have been produced by the leakage of energetic electron-photon component through the absorber above the detector or through the sides in case of showers arriving with large zenith angle. The diplot of the number of particles and the arrival delay for events of types B and C is shown in Fig. 8. Events of type B with two different delays from the two detectors are represented by two points in this diplot. Interestingly this diplot shows many events which have given large signal (>40 particles) and large delay (>20 ns) in one of the hadron detectors. The detailed charac-

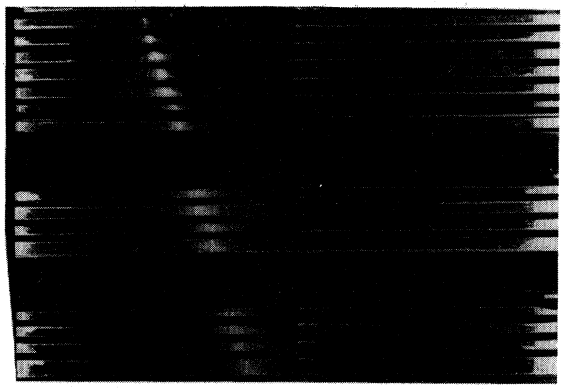

(a)

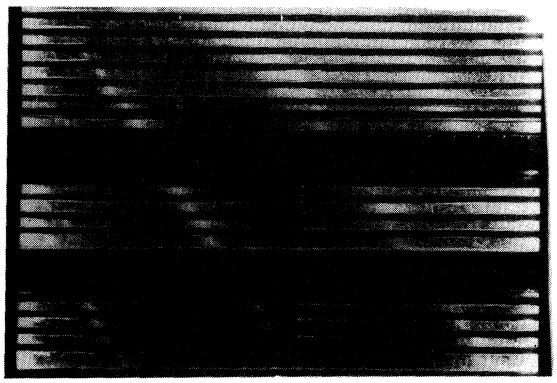

(b)

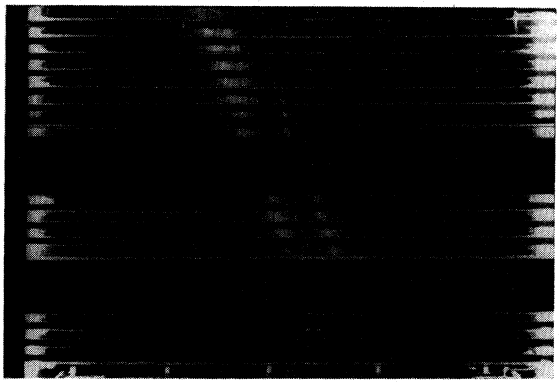

(c)

FIG. 7. Cloud-chamber pictures for (a) a type A event showing a single high-energy cascade, (b) a type A event showing two hadron cascades close to each other, and (c) a type C event showing the cascade missing the lower detector.

teristics for these special events are given in Table IV. The events labeled B(R) or C(R) in this table show clear evidence for the presence of two hadrons through the detector which are well separated in time. Since the hadron arriving earlier could

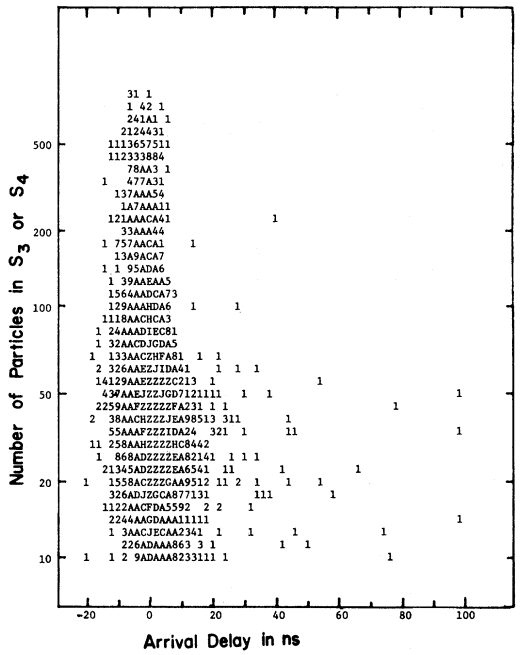

FIG. 8. Diplot of the number of particles and the arrival delay for types B and C events (part 1).

have given a maximum of 20-particle signal without affecting the time measured by the high-threshold channel, a few of these events may not have >40-particle signals from the delayed particle.

The events listed in Table IV show the surprising and rather unexpected feature that signals as large as 50—100 particles in one detector are not acccompanied by any signal at all in the other detector when the separation between the detectors is only 56 g cm^2 of absorber. Of course, a few events of type C could be expected due to the fact that the cascade traversed only one detector, missing the other detector as shown by the example in Fig. 7(c). More information about these rare events could not be obtained because none of these events except event No. 9 in Table IV have a cloud-chamber picture due to the chamber being nonoperational (recycling) at the time of these events. Two events, not listed in Table IV due to their somewhat lower energy but otherwise similar to the events listed in Table IV, did have chamber pictures. However both of these events [(i) 39 particles with 90 ns delay in S_3; (ii) 20 particles with 28 ns delay in S_3] showed no recognizable cascade in the chamber. In general only about 30% of the low-energy delayed events had recognizable cascades in the chamber picture.

TABLE IV. Characteristics of delayed energetic events of types B and C.

Serial number	Event identification number	$10^{-4}\times$Shower size	Shower density (m^{-2})	Shower core distance (m)	Shower arrival angle (deg)	Number of particles S_3	Number of particles S_4	Arrival delay (ns) S_{3L}	Arrival delay (ns) S_{3H}	Arrival delay (ns) S_{4L}	Arrival delay (ns) S_{4H}	Event type
1	87473	20	18	24	34	50	0	35	39			C
2	145195	43	40	17	31	67	0	17	22			C
3	154604	44	20	39	8	44	0	76	82			C
4	163287	84	116	14	28	2	47	5		20	22	B
5	199927	2	20	6	22	0	41			24	25	C
6	190912	20	10	9		50	0	0	31			C(R)
7	246441	31	180	6	13	61	0	4	28			C(R)
8	295859	999	440	21	6	14	47	0		131	135	B
9	384327	5	720	0	7	244	91	*[c]	40	*[c]	1	B
10	141282	7	6	14	15	42	8	24	*[c]	3	*[c]	B
11	195357	52	144	13	40	103	6	5	28	3		B(R)
12	280451	10	10	10	28	9	56	0		1	20	B(R)
13	284011	999	160	66	34	25	54	2		0	54	B(R)
14	338895	999	120	54		60	4	10	35	4		B(R)
15	150882	20	200	4	28	19	41	0		7	21	B(R)
16	237793	45	60	13	30	57	65	3	22	3	3	B(R)
17[a]	342411	na[b]	16	na[b]	na[b]	61	0	45	46			C
18[a]	352507	na[b]	12	na[b]	na[b]	73	0	23	24			C
19[a]	400170	na[b]	68	na[b]	na[b]	9	83	0		1	37	B(R)
20[a]	463096	na[b]	120	na[b]	na[b]	21	47	0		0	32	B(R)

[a]Events observed in part 2 of the experiment.
[b]Not analyzed.
[c]Channels not operational.

The details for event No. 9 (Table IV) can be seen from the chamber picture shown in Fig. 9. It shows a good hadron cascade which probably started in the iron-lead shielding above the chamber. Observed signals of 244 particles in S_3 and 91 particles in S_4 seem to be consistent with the structure of the cascade seen above the detectors. However this event has been timed as delayed (40 ns) by S_3 but prompt (1 ns) by S_4. Of course the incidence of a lower-energy prompt hadron, not seen clearly in the picture, could have triggered the timing channel for S_4 in a manner similar to that observed for some events, labeled B(R) or C(R), shown in Table IV. This possibility looks particularly attractive since the shower core for this event is very close ($\sim$2 m) to the cloud chamber. However, due to this ambiguity associated with this event, it cannot be considered as definite evidence for a high-energy delayed hadron.

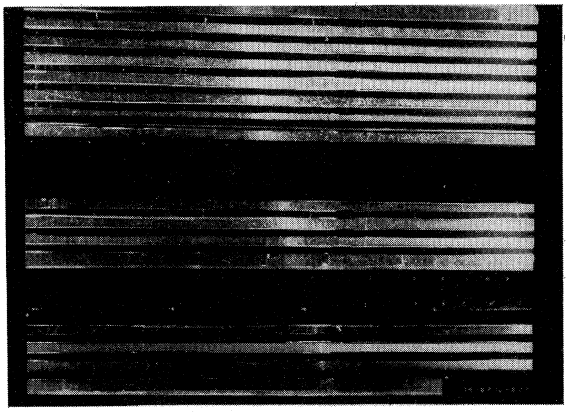

FIG. 9. Cloud-chamber picture for event No. 9 (Table IV).

C. Results from part 2 of the experiment

The results obtained from the data collected in the first part of the experiment have shown that there are no delayed energetic events which give delayed signal in both hadron detectors (type A) but that there are quite a few events among types

B and C which show a large delayed signal in only one of the detectors. Since there was a vertical separation of 60 cm between S_3 and S_4 with 56 g cm^{-2} of iron absorber between them, these results suggest that the observed delayed energetic events are probably due to some special type of interaction which gives a cascade with a very short absorption mean free path. Other possibilities are (i) for events close to the shower core the other detector is often triggered by other hadrons, and (ii) the hadron cascade has missed the other detector for these events. Since chamber observations show 47% of type A events to have more than one cascade over the hadron detector, multihadron incidence presents a definite and almost unavoidable problem for the detection of delayed energetic events. However, before speculating on the type of particle and its interaction which could simulate the observed events it is necessary to study these events with reduced separation between the hadron detectors. Therefore the vertical separation between S_3 and S_4 was reduced to 15 cm in the second part of the experiment. The absorber thickness between S_3 and S_4 was about 3 g cm^{-2}. It was not possible to reduce the separation further due to the necessity of making light-tight boxes for these two scintillators and due to the dimensions of the light guide toward the photomultipler end. The numbers and relative frequencies of different type of events observed in part 2 are given in Table II. As expected the relative frequency of type C events among those collected with lower particle threshold level has decreased from 65% in part 1 to 48% in part 2 due to the reduction in the spacing and the absorber thickness between the detectors. The change is even more dramatic for events collected with higher-threshold level since the relative frequency of type C events has decreased from 17% in part 1 to only 1% in part 2. Figure 10 shows the correlation between the delays measured by S_3 and S_4 for events collected in part 2. A comparison of the distribution of events in this figure with the distribution in Fig. 4 (part 1) reveals that the number of events lying on the diagonal (type A) has increased significantly relative to type B events lying along the axes. The diplots of the number of particles and the arrival delay for type A and for types B and C are shown in Figs. 11(a) and 11(b), respectively. It is seen that the distribution for type A events is very similar to that observed for events in part 1 except for the reduced width. There are no high-energy (>40 particles) delayed (>20 ns) events among the type A events

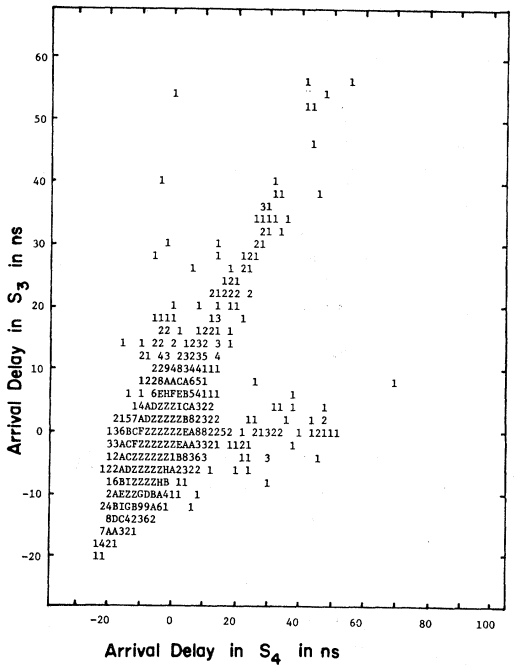

FIG. 10. Correlation between the delay of the signal in S_3 and S_4 (part 2).

but there are four events of this class among the types B and C events [Fig. 11(b)]. These events (Nos. 17–20 in Table IV) are very similar to those seen in part 1. There are no cloud-chamber pictures for these events.

IV. DISCUSSION

The experimental results presented in the preceding section have confirmed the existence of delayed energetic events of a kind similar to those seen in earlier experiments.[3–7] However, all the delayed energetic events seen in the present experiment are delayed in only one of the two hadron detectors, independent of the thickness of the absorber between these two detectors. This new and very significant information makes it very difficult to interpret these events to be due to normal high-energy hadronic interactions. This is due to the fact that the fluctuations in the development[11] of a hadron-electron-photon cascade are not expected to be so large as to give a signal of more than 40 particles in one detector and almost no signal in the other detector when the absorber thickness between these detectors is only 3 g cm^{-2}. The observation of this special feature of the delayed energetic events is consistent with observations reported

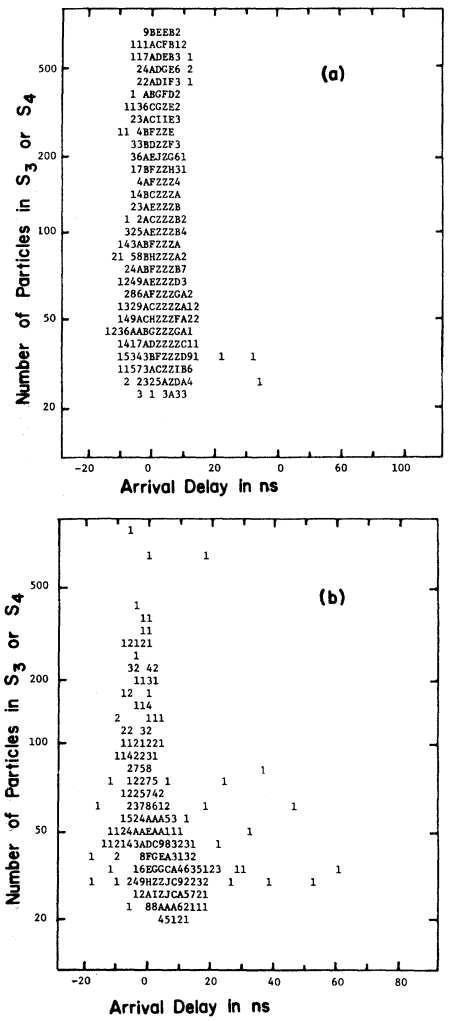

FIG. 11. Diplot of the number of particles and the arrival delay for (a) type A events and (b) types B and C events (part 2).

from earlier experiments.[3–7] For example, Jones *et al.*[4] and Tonwar *et al.*[5] have also observed almost all the delayed energetic events to be of a single detector type. The absorber thickness between the sampling layers of the calorimeter in the experiment of Jones *et al.*[4] was 60–120 g cm^{-2} (iron) and five of the six observed delayed energetic events gave signals in only one sampling layer. The absorber thickness between sampling layers of the calorimeter used by Tonwar *et al.*[5] was less (30 g cm^{-2}) but many sampling layers (6–8) were viewed together with a single photomultiplier. Tonwar *et al.*[5] observed ten delayed energetic events and most of the ionization for these events was recorded in one of the detector channels of the calorimeter. The experiments of Tonwar *et al.*[6] and Goodman *et al.*[7] were similar in that they used a single scintillation detector inside the absorber assembly to detect and time the delayed energetic events. Tonwar *et al.*[6] observed two events which showed well developed cascades in the cloud chamber. Goodman *et al.*[7] observed three delayed energetic events in their experiment. All these observations are summarized in Table V. It should be mentioned that events labeled B(R) or C(R) in Table IV have not been counted for the purpose of the comparison given in Table V.

The main characteristics of all the delayed energetic events observed in various experiments are also shown in Fig. 12. As seen from this figure and also Table V the flux and the characteristics of observed events in these experiments are very similar. The absence of the type A events among the observed events during the first part of the present experiment could be interpreted by assuming that the interactions responsible for these events produce a large number of low-energy particles which are rapidly absorbed in the absorber assembly. For example, such a large number of secondary particles could be expected for the interaction of a massive (>20 GeV/c^2) particle of total energy >500 GeV which loses only 10–20 % of its energy in the interaction. However, the absence of the type A events in the second part of the experiment rules out this possibility.

The presence of a large flux of low-energy hadrons in regions close to the shower core can possibly lead to a suppression of the detection probability for type A delayed energetic events. In fact, of the 20 events given in Table IV, 14 events (types B and C) clearly show the arrival of a low-energy particle earlier than the delayed signal in the same detector. However, the other 6 events show signals in only one detector suggesting that the flux of low-energy particles is not overwhelming. Although cloud-chamber observations[12] show that nearly half of the type A events have more than one hadron cascade over the detector area, there is only one delayed event (No. 9 in Table IV), which shows the presence of another high-energy hadron (in S_4). Of course, delayed energetic events which were preceded by prompt high-energy hadrons which could give large signal in both S_3 and S_4 would be recorded as prompt events in this experiment.

Thus there is no firm evidence from this experiment for the existence of delayed energetic events with a signature expected if the massive hadron had a normal interaction. Also the observed

TABLE V. Summary of results from various experiments.

Experiment	Detector area (m^2)	Exposure factor (m^2 yr)	Characteristics of observed events	Number of events	Rate (m^{-2} yr^{-1})
Jones *et al.* (Ref. 4)	1.60	0.28	Energy ≥ 30 GeV Delay ≥ 30 ns	6	21
Tonwar *et al.* (Ref. 5)	1.44	0.21	Energy ≥ 30 GeV Delay ≥ 28 ns	10	47
Tonwar *et al.* (Ref. 6)	0.36	0.12	Energy ≥ 30 GeV Delay ≥ 20 ns	2	17
Goodman *et al.* (Ref. 7)	0.56	0.61	Particles ≥ 40 Delay ≥ 20 ns	3	5
Bhat *et al.* (this paper)	0.64	0.85 Type A Parts 1 and 2	Particles ≥ 40 Delay ≥ 20 ns	0	0
		0.85 Type B Parts 1 and 2	Particles ≥ 40 Delay ≥ 20 ns	6	7
		0.53 Type C Part 1	Particles ≥ 40 Delay ≥ 20 ns	4	8
		0.41 Type C Part 2	Particles ≥ 40 Delay ≥ 20 ns	2	5

features for the delayed energetic events seen here clearly show that such events seen also in other experiments[3–7] need not be interpreted as due to a massive hadron. Since the exposure factor for the present experiment is the largest of all the experiments to date which have searched for massive particles in air showers, the results presented here can be used to obtain a sensitive upper limit for the cosmic-ray flux (ϕ_m) of massive particles (m GeV/c^2) with normal hadronic interaction characteristics associated with air showers. This upper limit is

$$\phi_m \leq 1.7\times 10^{-11}\ \text{cm}^{-2}\text{s}^{-1}\text{sr}^{-1} \text{ at } 99\%\ \text{C.L.}$$

This value is quite close to the expected flux $\sim 1.4\times 10^{-11}$ $\text{cm}^{-2}\text{s}^{-1}\text{sr}^{-1}$ given by the calculation of Isgur and Wolfram[13] for a particle of mass ~ 10 GeV/c^2. Using the relation between the cosmic-ray flux (ϕ_m) and the production cross section for a particle of mass m given by Jones,[8]

$$\sigma_m = 7\times 10^{-26} m^{3.33} \phi_m \text{ cm}^2 ,$$

an upper limit for the production cross section (σ_m) for particles of mass $m \geq 10$ GeV/c^2 can be obtained as

$$\sigma_m \leq 2.5\times 10^{-33}\ \text{cm}^2$$

for interactions at energies of $10^5 - 10^7$ GeV. The accelerator experiments[14] have placed an upper limit of $\sim 10^{-36}$ cm^2 for the production cross section for particles of mass in the $4-10$ GeV/c^2 range for proton-proton interactions at an energy of 400 GeV.

Notwithstanding these results for the upper limits on the flux and the production cross section of massive particles in cosmic-ray interactions in the atmosphere, obtained from the bulk of the data in

the present experiment, it should be emphasized here that it is difficult to interpret the delayed energetic events which have shown well-developed cascades in the cloud chamber (one in the present experiment and two in the experiment of Tonwar *et al.*[6]). Since the sensitive time of the chamber is several tens of milliseconds it was suggested[15] that the delayed events seen by Tonwar *et al.*[6] may be due to a chance coincidence of an unrelated hadronic cascade in the chamber with the delayed trigger. The number of events expected due to chance can be calculated as

N_{chance} = (observed rate of delayed events)
× (observed rate of hadrons of energy > 50 GeV over the detector area at the observational level)
× (coincidence time) × (observation time) .

Taking the observed rate of delayed energetic events from the present experiment (more than 10 particles and delays larger than 30 ns) as about 30 in 6000 h, the hadron rate as 1 per h, the sensitive time as 50 ms and the observation time as 3000 h (Tonwar *et al.*[6]),

$$N_{\text{chance}} \sim 2.1 \times 10^{-3} .$$

Thus the events seen by Tonwar *et al.*[6] are unlikely to be due to the chance coincidence of this type. The number of events expected due to chance in the present experiment is only about 10^{-7} since 150 ns has to be used as the coincidence time. This is due to the fact that the gate width for the ADC module is 150 ns and the number of particles recorded in S_3 and S_4 for the delayed event agree well with the numbers estimated from the chamber picture. It is unfortunate that due to various operational problems there are no chamber pictures for other observed events. However, it seems clear that more observations with cloud chamber for the delayed energetic events should help in clarifying the situation and may provide interesting information.

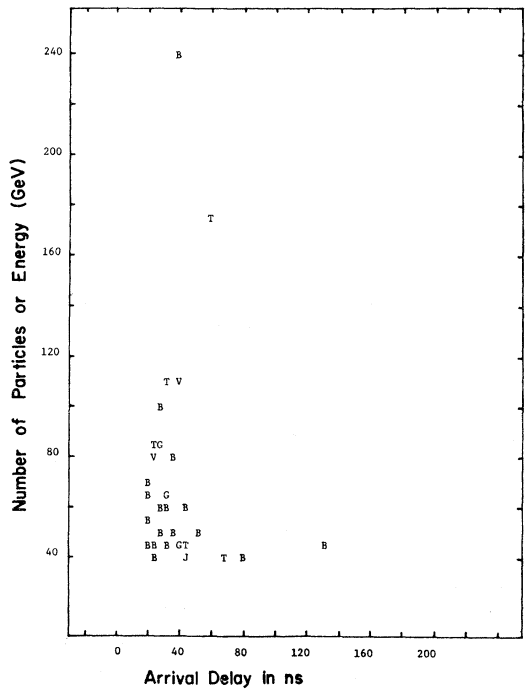

FIG. 12. Diplot of the number of particles (or energy) and the arrival delay for the delayed energetic events observed in different experiments. J, Jones *et al.* (Ref. 4); T, Tonwar *et al.* (Ref. 5); V, Tonwar *et al.* (Ref. 6); G, Godman *et al.* (Ref. 7); B, Bhat *et al.* (this experiment).

It should be remarked that the energetic events listed in Table III, although only marginally delayed, are also difficult to understand in terms of normal particles since clean cascades are seen for some of these type A events in the chamber pictures. However, since the delays are only in the 10–15 ns range it is difficult to rule out the possibility that these delays are not due to the extreme fluctuation in the arrival time measured by the shower detectors. For example, for the most significant event (No. 5 in Table III), it is seen that there is a difference in the arrival time between S_1 and S_2 of 9 ns. The hadron delay as given in Table II is the one measured relative to the earlier of the two signals. However, these observations suggest that a search for very energetic events with small delays may also yield interesting results.

It is interesting to speculate on the nature of particles responsible for the observed delayed energetic events of type C, particularly those observed during part 2 of the experiment. It is clear that these events are due to either low-energy hadrons which deposit most of their energy in 1–2 g cm^{-2} of absorber or due to some new process. While low-energy (~1 GeV) neutrons emitted as nuclear

fragmentation products in hadron-nucleus collisions occurring in air showers could be considered as a possible source for some of these events, a qualitative comparison of the delay-energy characteristics and considerations of the flux required suggest the neutrons to be the unlikely candidate for the particles producing these events. An experimental study of events expected due to low-energy neutrons being planned by Goodman *et al.*[16] might provide relevent information on the nature of the observed delayed events.

Finally it is relevant to note here that almost all the experiments searching for the production of massive particles in air showers (including the present one) which have used the large delay and high energy as the signature for the large mass require the particles to have the following general characteristics: (i) The lifetime should be larger than 10^{-6} s to allow the particle to travel a distance of about a kilometer or more in the atmosphere, (ii) the interaction cross section of these particles for various nuclei should be comparable to that of known hadrons such as nucleons, pions, etc., (iii) the inelasticity in interactions of these particles should have a value larger than about 0.1 for them to be detectable as a high-energy particle, and (iv) some of these particles or their progeny should be found at larger distances, more than about 3 m, from the shower core at the observational level since the presence of a large density of high-energy hadrons close to the core makes it difficult to detect the delayed particles.

V. CONCLUSIONS

The experimental results obtained in the present experiment have clearly shown the presence of delayed energetic events of a similar kind as seen in earlier experiments.[3–7] However, a study of the details of these events made possible by better instrumentation has shown that these events cannot be interpreted as due to conventional high-energy hadronic interactions. Therefore it can be concluded that there is no evidence from the bulk of the data for the existence of delayed high-energy hadrons with normal interaction which could be interpreted in terms of production of massive particles in high-energy interactions occurring in the cores of extensive air showers. A 99% C.L. upper limit of 1.7×10^{-11} cm^{-2}s^{-1}sr^{-1} has been obtained for the flux of massive particles of mass ≥ 10 GeV/c^2 which is quite comparable to the flux expected from theoretical considerations.[13] Using this upper limit on flux, an upper limit on the production cross section for particles of mass ≥ 10 GeV/c^2 in high-energy interactions can be obtained as $\sim 2.5\times10^{-33}$ cm^2. It should be emphasized that these values are applicable only for particles with certain well defined characteristics as discussed earlier.

Further experimental investigation is required to understand the nature of particles responsible for the observed delayed energetic events which are seen to deposit most of the large amount of ionization in or near one of the hadron detectors. Interpretation of these events as due to low-energy neutrons, although plausible, is not free of difficulties. In this experiment also one well developed cascade has been seen in a cloud-chamber picture for a delayed energetic trigger, similar to the observation of two delayed cascades by Tonwar *et al.*[6] Interpretation of these events in terms of normal hadronic phenomenon seems to be very difficult and only more observations of many such events may provide some definitive answer as to the nature of particles responsible for these events.

ACKNOWLEDGMENTS

It is a pleasure to acknowledge technical assistance from A. R. Apte, N. V. Gopalakrishnan, J. A. Joshi, S. Ramani, R. Mahalingam, and S. Y. Tandale.

---

*Present address: Department of Physics and Astronomy, University of Maryland, College Park, Maryland 20742.

[1]M. Gell-Mann, Phys. Lett. 8, 214 (1964); G. Zweig, Report No. CERN-TH 412, 1964 (unpublished); M. Y. Han and Y. Nambu, Phys. Rev. B 139, 1006 (1965); J. C. Pati, and A. Salam, Phys. Rev. D 10, 275 (1974); V. Elias, J. C. Pati, and A. Salam, Phys. Rev. Lett. 40, 920 (1978), and others.

[2]G. Damgaard *et al.*, Phys. Lett. 17, 152 (1965).

[3]B. K. Chatterjee, G. T. Murthy, S. Naranan, B. V. Sreekantan, M. V. Sreenivasa Rao, and S. C. Tonwar, in *Proceedings of the Ninth International Conference on Cosmic Rays,* edited by A. C. Stickland (The Insti-

tute of Physics and the Physical Society, London, England, 1965), Vol. 2, p. 805.
[4]L. W. Jones *et al.*, Phys. Rev. 164, 1584 (1967).
[5]S. C. Tonwar, S. Naranan, and B. V. Sreekantan, J. Phys. A 5, 569 (1972).
[6]S. C. Tonwar, B. V. Sreekantan, and R. H. Vatcha, Pramana 8, 50 (1977).
[7]J. A. Goodman, R. W. Ellsworth, A. S. Ito, J. R. MacFall, F. Siohan, R. E. Streitmatter, S. C. Tonwar, P. R. Viswanath, and G. B. Yodh, Phys. Rev. D 19, 2572 (1979).
[8]L. W. Jones, Rev. Mod. Phys. 49, 717 (1977).
[9]S. C. Tonwar, G. T. Murthy, and B. V. Sreekantan, Proc. Indian Acad. Sci. 74, 203 (1971).
[10]For example, J. Engler *et al.*, Nucl. Instrum. Methods 106, 189 (1973); H. Whiteside *et al.*, *ibid.* 109, 375 (1973); M. Holder *et al.*, *ibid.* 151, 69 (1978).
[11]R. H. Vatcha, B. V. Sreekantan, and S. C. Tonwar, J. Phys. A 5, 859 (1972).
[12]B. V. Sreekantan and S. C. Tonwar, in *Sixteenth International Cosmic Ray Conference, Kyoto, 1979, Conference Papers* (Institute of Cosmic Ray Research, University of Tokyo, Tokyo, 1979), Vol. 8, p. 287; B. V. Sreekantan, S. C. Tonwar, and P. R. Viswanath, in *17th International Cosmic Ray Conference, Paris, 1981, Conference Papers* (Centre d'Etudes Nucleaires, Saclay, 1981), Vol. 6, p. 198; S. C. Tonwar, *ibid.*, Vol. 13, p. 325.
[13]N. Isgur and S. Wolfram, Phys. Rev. D 19, 234 (1979).
[14]For example, D. Cutts *et al.*, Phys. Rev. Lett. 41, 363 (1978).
[15]C. B. A. McCusker, Phys. Rep. 20C, 229 (1975).
[16]J. A. Goodman, A. Mincer, S. C. Tonwar, G. B. Yodh, and R. W. Ellsworth, in *17th International Cosmic Ray Conference, Paris, 1981, Conference Papers* (Ref. 12), Vol. 5, p. 36.

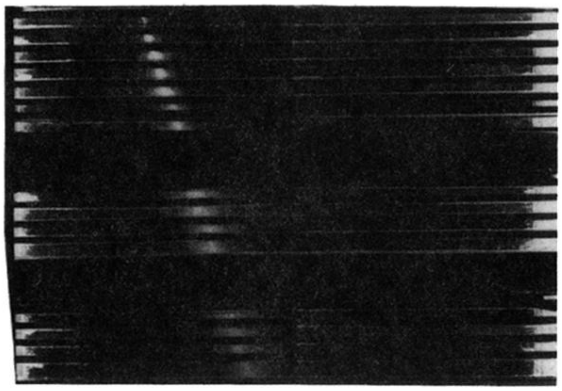

(a)

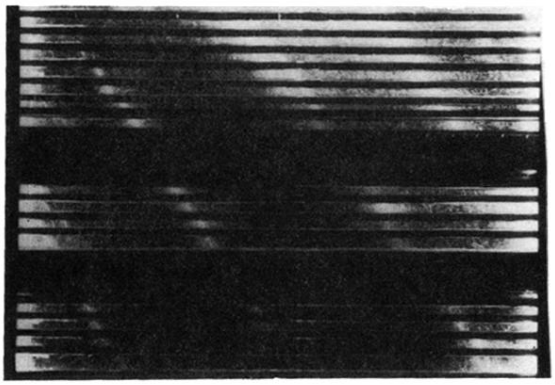

(b)

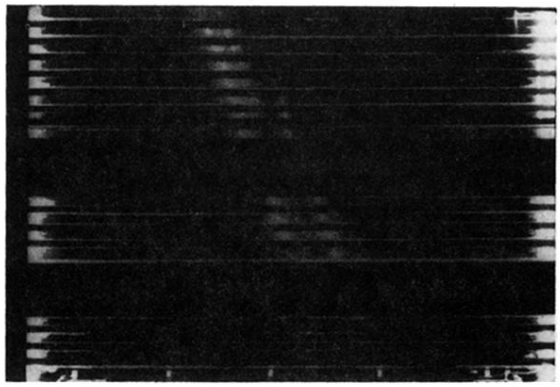

(c)

FIG. 7. Cloud-chamber pictures for (a) a type A event showing a single high-energy cascade, (b) a type A event showing two hadron cascades close to each other, and (c) a type C event showing the cascade missing the lower detector.

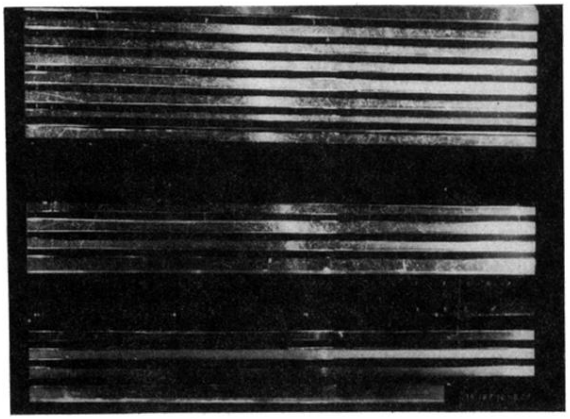

FIG. 9. Cloud-chamber picture for event No. 9 (Table IV).